

Improving Transferability for Domain Adaptive Detection Transformers

Kaixiong Gong¹ Shuang Li^{1†} Shugang Li¹ Rui Zhang¹ Chi Harold Liu¹ Qiang Chen²

¹Beijing Institute of Technology ²Baidu VIS

{kxgong, shuangli, shugangli, zhangrui20}@bit.edu.cn
liuchi02@gmail.com, chenqiang13@baidu.com

Abstract

DETR-style detectors stand out amongst in-domain scenarios, but their properties in domain shift settings are under-explored. This paper aims to build a simple but effective baseline with a DETR-style detector on domain shift settings based on two findings. For one, mitigating the domain shift on the backbone and the decoder output features excels in getting favorable results. For another, advanced domain alignment methods in both parts further enhance the performance. Thus, we propose the Object-Aware Alignment (OAA) module and the Optimal Transport based Alignment (OTA) module to achieve comprehensive domain alignment on the outputs of the backbone and the detector. The OAA module aligns the foreground regions identified by pseudo-labels in the backbone outputs, leading to domain-invariant based features. The OTA module utilizes sliced Wasserstein distance to maximize the retention of location information while minimizing the domain gap in the decoder outputs. We implement the findings and the alignment modules into our adaptation method, and it benchmarks the DETR-style detector on the domain shift settings. Experiments on various domain adaptive scenarios validate the effectiveness of our method.

1. Introduction

DETR-style detectors [3, 51] remove hand-craft designs in the standard in-domain scenarios and offer promising performance. However, the domain shift scenarios with changing weather, varying illumination, and altering scene layout are more related to reality. In this paper, we aim to extend the application scenarios of DETR-style detectors by creating a simple but effective baseline for domain adaptive object detection (DAOD).

In DAOD, methods and recipes for DETR-style detectors are yet to be built, compared with the well-established CNN-based detectors. That brings us back to the basics, and asks the question: *where and how to adapt with DETR-style*

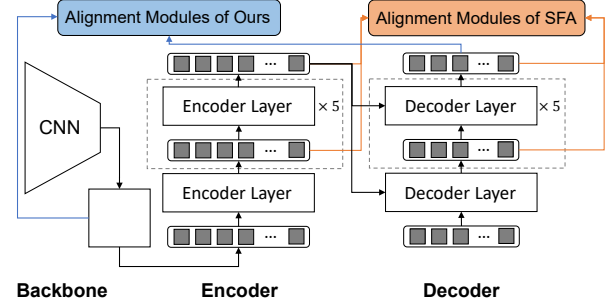


Figure 1. Overview of the alignment paradigms of ours and SFA [42]. Ours aligns the output features of CNN backbone and decoder. While SFA aligns the token embeddings of each layer of encoder and decoder.

detectors?

Wang et al. [42] made their practice, advocating aligning the sequence token embeddings of each layer of encoder and decoder, demonstrating the potential of detection transformers in the domain adaptive setting, as shown in Fig. 1. Nonetheless, we argue that it’s cumbersome and sub-optimal to align the embeddings of each layer of encoder and decoder.

The first concern is about “where”. Detection transformer is composed of three main modules: a CNN backbone to extract the feature representations from raw images, an encoder for feature enhancement, and a decoder to probe features for following locating and classification. Among them, the CNN backbone directly processes the images, whose features will be served as the input of the subsequent transformer. As a result, the quality of the CNN features is the cornerstone of the following process by the transformer. Thus, it’s essential to align the features of the CNN backbone for domain-invariant backbone features. On the other hand, the role of the encoder is to enhance the CNN features using the attention mechanism for better feature probing by the decoder. Since we have aligned the backbone features and transformer networks are not non-trivial to train [40, 51], there is no strong need to align the token embeddings of the encoder during the feature enhancement stage. Finally, the decoder adopts object queries to probe image

[†]Shuang Li is the corresponding author.

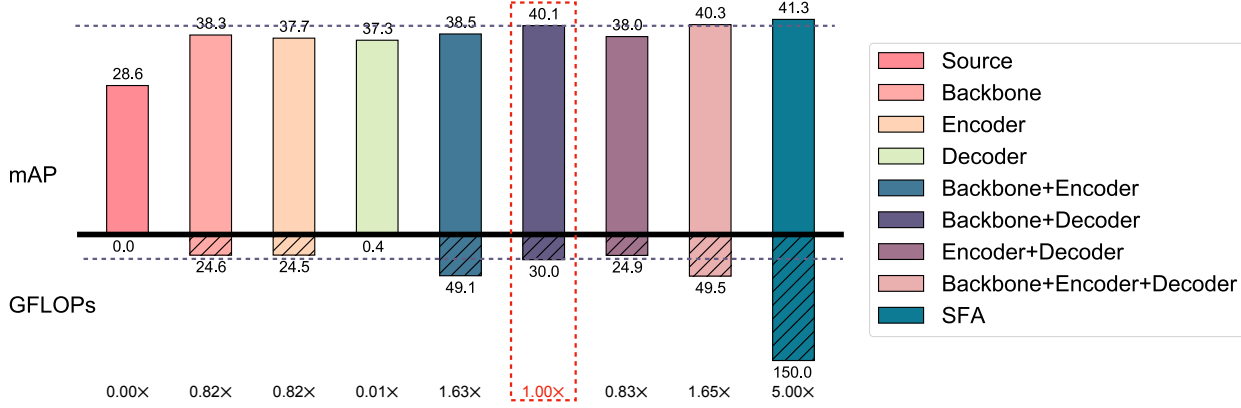


Figure 2. The top shows the mAPs of different variations on Cityscapes \rightarrow Foggy Cityscapes, while the bottom presents the extra computational cost of these variations by excluding the overhead of the based detector. “Source” denotes the basic Deformable DETR model [51]. “Backbone”, “Encoder” and “Decoder” denote aligning the multi-scale features of the CNN backbone, the output features of encoder and decoder via adversarial training [14], respectively. The rest variations denote unifying any two or all alignment modules for training. This work adopts the “Backbone+Decoder” scheme (highlighted with the red dash) at the consideration of performance and overhead.

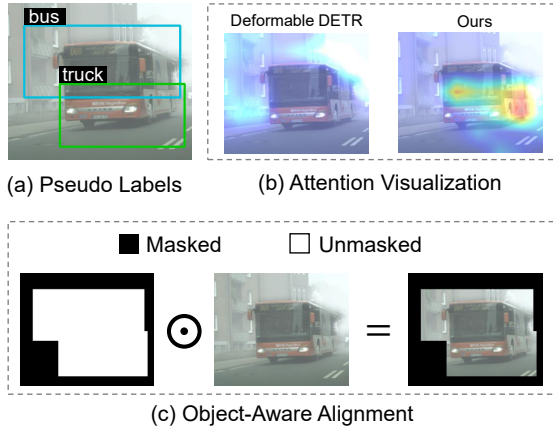


Figure 3. (a): Cases of inaccurate pseudo labels, misclassification (green box) and mislocation (green and blue boxes). (b): Attention visualizations for target samples of source model and our method. Ours facilitates the CNN backbone concentrating on the discriminative regions via Object-Aware Alignment, while the attention of the source model is biased to the background area. (c): Illustration of Object-Aware Alignment (OAA). The pixels of the feature map enclosed by the pseudo bounding boxes will be highlighted during alignment. We use the pseudo labels in a class-agnostic manner. The cooperation of two inaccurate pseudo bounding boxes might be still able to discover the object. Consequently, OAA can reduce the negative effect of inaccurate pseudo labels and make full use of them.

features for detection, whose output features are directly utilized for locating and classification. Hence, the decoder features are critical for detection performance. However, unfortunately, the features of the decoder are inevitably biased to the source domain due to the absence of supervision from the target domain. To tackle this issue, we follow [46][‡]

[‡]It suggests that the features of deeper layers are more transferable.

and propose to align the output features of the decoder instead of the token embeddings of each layer.

We empirically support this claim by conducting comparison experiments of various alignment scheme variations, as shown in Fig. 2. Only aligning the features of any of the three modules obtains unsatisfactory performance gains. Take a step further, unifying any two alignment schemes, e.g., “Backbone+Encoder” and “Backbone+Decoder”, leads to enhanced results. Furthermore, one can observe that backbone alignment is essential for overall performance, while the alignment for encode features is not necessary.

The second concern is about “how”. SFA [42] exploits adversarial learning for aligning the token embeddings of each layer of decoder. Although being effective, adversarial alignment might distort the intrinsic distribution characteristics [5]. In the case of decoder alignment, this adversarial scheme might damage the crucial location information, which limits the performance of detectors.

To tackle this, we propose an Object-Aware Alignment (OAA) module for acquiring domain-invariant backbone features. Plainly conducting alignment on the global backbone features can narrow the domain gap between domains. Such a coarse-grained alignment strategy is effective, but ignores the difference between the objects and background. The regions containing objects should be emphasized during alignment, since they are more transferable than the background regions, as the domain shift is usually presented in the background. In light of this, we introduce a simple yet effective scheme, utilizing the pseudo labels to identify the foreground regions, which is complementary to the global alignment. Concretely, the pixels of feature maps enclosed by pseudo bounding boxes will be highlighted during alignment. As a result, the detector will concentrate on

the object area of target samples as illustrated in Fig. 3(b). Prior works generally leverage the pseudo labels for self-training [22, 20], which requires highly reliable pseudo labels to avoid the negative transfer. As illustrated in Fig. 3, when the pseudo labels are inaccurate, self-training might harm the detector performance. While, in OAA, we utilize the pseudo labels in a class-agnostic manner. Hence, the noisy pseudo labels can still be helpful to identify the desired regions that contain objects, leading to comprehensive backbone feature alignment.

On the other hand, not only the backbone features are severely biased by the domain shift, so as the features of the decoder, due to the absence of supervision from the target domain. The features of the decoder carry important location information, which is crucial for final predictions. Hence, how to reduce the domain gap while simultaneously maintaining the location characteristics is critical for domain adaptive detection transformers. Instead of applying adversarial learning, we resort to Wasserstein Distance, which takes into account the intrinsic geometry information. Concretely, Wasserstein Distance seeks an optimal transport plan for moving one distribution to another with minimal cost. Thus, adopting it to mitigate the discrepancy of the decoder features between source and target domain might be able to maximumly preserve the location information. Nonetheless, the complexity of approximating Wasserstein Distance in the high-dimensional space (the feature space) is intolerable. To overcome this, we utilize sliced Wasserstein Distance, solving several one-dimensional optimal transport problems by projecting the decoder features to one-dimensional space, which have closed-form solutions. Thus, the detector can be efficiently trained and the location information is reversed. Consequently, our method yields more highly accurate bounding boxes as verified in Section 4.5. Extensive experiments on several adaptive benchmarks manifest that our method consistently enhances the detection performance on new domains of the DETR-style detector and surpasses various competitive approaches.

In summary, the main contributions of this work are:

1. We discovered that mitigating domain shift on the output features of CNN backbone and decoder yields favorable results with cost-efficient computational overhead.
2. We propose two alignment modules: an Object-Aware Alignment module for obtaining domain-invariant backbone features and an Optimal Transport based Alignment (OTA) module for reducing the domain shift on decoder features.
3. Extensive experiments on several adaptation benchmarks validate the effectiveness of our method.

2. Related Work

In this section, we discuss the prior works related to ours.

Object detection. Object detection, involving locating and classification, is an essential task in computer vision. In the early years, CNN-based detectors dominated the object detection community, which can be roughly divided into two categories: two-stage [33] and one-stage detectors [32, 30]. Two-stages detectors first generate proposals with selective search [15] or region proposal network [33], then produce detections by refining the proposals. One-stage detectors instead skip generating proposals and directly predict detection results from images, thus enjoying faster inference speed.

Recently, a transformer-based detector, DETR, [3] is introduced to achieve fully end-to-end detection and eliminate the hand-craft designed components, such as anchor generation and non-maximum suppression, which attracts a surge of research interest. Following, Deformable DETR [51] develops a sparse attention module named deformable attention to fasten the convergence speed of DETR. Sharing the same spirit, many researchers [9, 26, 48, 29] proposed various schemes to speed up the convergence of DETR. More recently, Wang et al. pointed out that DETR has the issue of data hunger and proposed to solve it by augmenting the supervision. Nonetheless, how to enhance the generalization ability of the DETR-style models to new domains has not been fully explored yet. In this work, we delve into enhancing the transferability of DETR-style models.

Domain adaptive object detection. DAF [6] is the first work attempting to transfer the object detector across domains, which proposes to align the backbone and the ROI features. Inspired by it, researchers are devoted to boost the transferability of detectors by improving feature alignment schemes [35, 50, 45, 44, 17, 23, 19, 34, 4, 49]. SWDA [35] proposes to employ strong alignment on the local features while weak alignment on the global features of the CNN backbone. Zhang et al. introduce learnable RPN prototypes for aligning the RPN features of source and target domains. MTOR [2] and UMT [12] exploit the teacher-student regime to overcome domain shift. While above works are designed for Faster RCNN [33], some other approaches are built on one-stage detectors [22, 18].

With the rising of DETR-style detectors [3, 51], Wang et al. advocate aligning the token embeddings of each layer of encoder and decoder for improving the cross-domain performance of them. Different from it, we find out that aligning the output features of CNN backbone and decoder yields favorable results and leads to cost-efficient computational overhead. In light of this, we propose two modules for mitigating the domain gap on the output features of CNN backbone and decoder.

Pseudo labels. Adopting pseudo labels for training is frequent in domain adaptation. Typically, the algorithms

leverage the confident target prediction for calibrating the parameters of classifiers, leading to better conditional distribution alignment [52, 43]. Further, [27, 28] refine the pseudo labels via clustering the target data for domain adaptation recognition. This is infeasible in detection transformers, since the features of the decoder contain important location information and have no intrinsic cluster property. In the context of domain adaptive object detection, some prior works [22, 20] also utilize the pseudo bounding boxes and classification results for self-training detectors, which heavily relies on the quality of pseudo labels. By contrast, we adopt the pseudo labels to mine the foreground regions, so as to put more attention on the objects during alignment. Furthermore, our method is more robust for noisy pseudo labels as illustrated in Fig. 3.

Optimal transport. Optimal transport has been applied in domain adaptation for transforming the source distribution to the target one [13, 8, 10]. The prior works [13, 8, 10] attempt to reach an optimal transport plan of aligning the distribution of two domains with theoretical guarantees. Derived from optimal transport theory, Wasserstein Distance (WD), is a metric that measures the minimal cost of the optimal transport problem, which has been used in generative adversarial nets [1] and domain adaptation [37]. Since it's non-trivial to directly approximate the WD in high-dimensional space, sliced Wasserstein Distance (SWD) [31] is then proposed to solve the optimal transport problems in the one-dimensional space via projecting the original vectors to one-dimensional space, which enjoys the geometry property of Wasserstein Distance and efficient training. Chen et al. [25] introduce SWD to domain adaptation for enforcing the consistent predictions of two task-specific classifiers. Different from them focusing on the image recognition task, we concentrate on the object detection task involving regression and classification, and propose two alignment modules for mitigating the domain gap on the output features of the CNN backbone and the decoder. To the best of our knowledge, we are the first to introduce SWD for reducing the domain gap in DAOD.

3. The Proposed Method

In this section, we present our proposed method. We start by introducing the problem setting and the based detector. In the context of domain adaptive object detection (DAOD), we can access a set of labeled source data $D_s = \{\mathbf{x}_i^s, Y_i^s\}_{i=1}^{n_s}$, where \mathbf{x}_i^s is the source image, $Y_i^s = \{(b_i^1, c_i^1), (b_i^2, c_i^2), \dots, (b_i^{m_i}, c_i^{m_i})\}$ is the annotation set containing m_i bounding boxes b_i^s and corresponding categories c_i^s . Meanwhile, the target domain only includes fully unlabeled target data $D_t = \{\mathbf{x}_i^t\}_{i=1}^{n_t}$. Since the weather, illumination and layout vary across domains, there exists crucial domain shift that hinders the performance on target domain. The goal of DAOD is to enhance the generalization

performance of detectors on the target domain using labeled source data and unlabeled target data.

In this work, we build our method on the Deformable DETR [51], which consists of a CNN backbone network for extracting based features, an encoder for feature enhancement, a decoder for feature probing, and finally feed-forward network (FFN) for prediction. In order to better detect small objects, Deformable DETR exploits the multi-scale features of the CNN backbone, where the small objects are detected from the high-resolution features. Let $\{f^l\}_{l=1}^L$ denotes the l^{th} level of feature, where $f^l \in \mathbb{R}^{C^l \times W^l \times H^l}$. In the following, the multi-scale backbone features will be flattened, embedded, and enhanced with positional and level embeddings [51] to construct sequence input for the transformer. Encoder further refines the features using the attention mechanism. Learnable object queries are utilized to probe the encoder features for detecting objects in decoder. Finally, FFN predicts the bounding boxes and categories of objects based on the decoder features.

As discussed in Section 1, the quality of backbone features directly affects the following process by the transformer. Thus, it's essential to align the features of the backbone, mitigating the negative influence of the domain gap. On the other hand, the output features of the decoder are directly utilized for location regression and category classification. Hence, the decoder features are crucial for the final detection performance. However, unfortunately, the features of the decoder are inevitably skewed to the source domain due to the absence of the supervision from target domain. To remedy these issues, we propose two alignment modules: an Object-Aware Alignment (OAA) module for CNN backbone features and an Optimal Transport based Alignment (OTA) module for decoder features.

3.1. Object-Aware Alignment

Domain-invariant backbone features are crucial for detection transformers, which will ease the domain shift issue. In Deformable DETR, the multi-scale backbone features are applied to improve the detection performance for small objects. Likewise, in order to better detect the small objects of the target domain, we establish feature alignment on multi-scale backbone features. The features of different level $\{f^l\}_{l=1}^L$ are fed into a domain discriminator, generating the domain scores for each pixel. If we denote the $P^l = \{p_i^l \in \mathbb{R}^{W^l \times H^l} | i = 1, 2, \dots, n_s + n_t\}$ as the discriminator outputs for l^{th} level of backbone features, we can formulate the adversarial training objective on l^{th} level features of backbones as:

$$\mathcal{L}_d^l = \sum_{i,u,v} \log(p_i^{s(u,v)}) + (1 - \log(p_i^{t(u,v)})), p_i^s, p_i^t \in P^l, \quad (1)$$

where the $p_i^{s(u,v)}, p_i^{t(u,v)}$ denote the discriminator outputs for source and target images located at (u, v) , respectively. Based on Eq. (1), we could define the alignment objective on multi-scale features:

$$\mathcal{L}_d = \sum_{l=1}^L \mathcal{L}_d^l. \quad (2)$$

To align the backbone feature distributions, the domain discriminator is optimized to minimize Eq. (2), while the backbone is updated for maximizing it. This global alignment strategy indeed can be beneficial to mitigate the domain gap between source and target domains. However, in the context of detection, this alignment scheme is insufficient, since 1) the foreground regions should be emphasized for reducing false negative detections and 2) the foreground regions are more transferable than the background ones, since the domain gap is usually presented in the background regions. Thus, we further utilize the predictions of FFN to highlight the discriminative regions that contain objects, since no region proposals are available in detection transformers. In other words, we encourage the detector to concentrate on the regions bounded by the predicted boxes. Former works typically adopt the pseudo labels for self-training, which might lead to error accumulation due to misclassification and mislocation issues. As we adopt the pseudo labels for feature alignment in a class-agnostic manner, the negative effect of the errors could be mitigated, as shown in Fig. 3.

Technically, let $\hat{Y}_i^t = \{(\hat{b}_i^1, \hat{s}_i^1), (\hat{b}_i^2, \hat{s}_i^2), \dots, (\hat{b}_i^{m_i}, \hat{s}_i^{m_i})\}$ denote the predicted results for i^{th} target image, where \hat{s}_i^j is the confidence score for j^{th} detection result. Note that we abuse the notation m_i here for simplicity. For acquiring confident detections, a threshold τ is utilized to filter the pseudo labels. Consequently, we obtain a pseudo bounding box set $\hat{B}_i^t = \{\hat{b}_i^j | \hat{s}_i^j > \tau, (\hat{b}_i^j, \hat{s}_i^j) \in \hat{Y}_i^t\}$ for i^{th} target image, which is exploited as the indicator for re-weighting the importance of each pixel of target backbone features:

$$w_i^{t(u,v)} = \begin{cases} 1, & \text{if } (u, v) \text{ located within } \hat{B}_i^t, \\ 0, & \text{else.} \end{cases}$$

The weights are utilized to encourage the backbone network to focus on those foreground areas and learn the patterns of objects across domains. Likewise, we directly exploit the ground truth bounding boxes of source samples to generate weights for source samples. Unifying the weights with alignment loss, we fulfill object-aware alignment:

$$\begin{aligned} \hat{\mathcal{L}}_d^l = & \sum_{i,u,v} w_i^{s(u,v)} \log(p_i^{s(u,v)}) \\ & + w_i^{t(u,v)} (1 - \log(p_i^{t(u,v)})), p_i^s, p_i^t \in P^l. \end{aligned} \quad (3)$$

Via aggregating $\hat{\mathcal{L}}_d^l$ on each level of features, we acquire $\hat{\mathcal{L}}_d$ for performing object-aware alignment on multi-scale features. On the basis of global alignment loss, we build the object-aware alignment loss. The two losses are used for adapting backbone features, as they are complementary to each other. Global alignment narrows the gap for better pseudo labels, while the region alignment improves detection for foreground objects. The loss of OAA module is:

$$\mathcal{L}_{OAA} = \mathcal{L}_d + \lambda \hat{\mathcal{L}}_d, \quad (4)$$

where λ is a trade-off hyper-parameter to balance the contributions of the two losses.

3.2. Optimal Transport Based Alignment

The features produced by decoder are directly utilized for predicting the location and category, which are critical for the detection performance. Although aligning the CNN backbone features can remedy the domain shift. But, the decoder is inevitably biased towards the source domain. Importantly, the features of decoder carry location information that is critical for the final detections, while adversarial training might distort the intrinsic distribution characteristics [5].

Hence, to reduce the domain shift and simultaneously preserve the location information, we resort to Wasserstein Distance, a metric derived from optimal transport theory, calculating the minimal cost of transporting a distribution to another. Wasserstein Distance seeks an optimal transport plan and leverages it to measure the cost. Formally, if we denote two random variables $z_1, z_2 \in \mathbb{R}^d$, a set of all joint distributions $\gamma(z_1, z_2)$ as $\Gamma(\mu, \nu)$. $\gamma(z_1, z_2)$ indicates that how much ‘‘mass’’ is transported from z_1 to z_2 for converting distribution μ to ν . The Wasserstein Distance can be formulated as:

$$W(\mu, \nu) = \inf_{\gamma \in \Gamma(\mu, \nu)} \int_{\gamma} c(z_1, z_2) d\gamma(z_1, z_2), \quad (5)$$

where $c(\cdot, \cdot)$ is the cost function, such as Squared Euclidean distance.

However, it’s non-trivial to estimate the optimal transport plan γ^* in the high-dimensional space, i.e., the feature space. To overcome this, sliced Wasserstein Distance (SWD) is utilized [31] for approximating the Wasserstein Distance, which solves optimal transport problems in the one-dimensional space via projecting the features to it. In specific, we sample K^{\S} projection vectors from a unit sphere $\mathbb{S} = \{\theta \in \mathbb{R}^d | \|\theta\| = 1\}$, where d is the dimension of decoder features. Then, these projection vectors will be exploited to project the decoder features to one-dimensional space. Let $f_{dec} = \{f_{dec}^1, f_{dec}^2, \dots, f_{dec}^N\}$ denote the decoder

^{\S}We set $K = 256$.

Table 1. Results on synthetic to real adaptation scenario, i.e., Sim10k \rightarrow Cityscapes. D-DETR denotes Deformable DETR [51].

Method	Detector	car AP
Faster RCNN (source)	Faster RCNN	34.6
DAF [6]	Faster RCNN	41.9
DivMatch [23]	Faster RCNN	43.9
SWDA [35]	Faster RCNN	44.6
SCDA [50]	Faster RCNN	45.1
MTOR [2]	Faster RCNN	46.6
CR-DA [44]	Faster RCNN	43.1
RPA [49]	Faster RCNN	45.7
CR-SW [44]	Faster RCNN	46.2
GPA [45]	Faster RCNN	47.6
VISGA [34]	Faster RCNN	49.3
D-adapt [20]	Faster RCNN	53.2
FCOS (source)	FCOS	42.5
EPM [18]	FCOS	47.3
KTNet [38]	FCOS	50.7
Deformable DETR (source)	D-DETR	47.4
SFA [42]	D-DETR	52.6
Ours	D-DETR	54.1

features, the SWD of source and target domains is defined as:

$$\mathcal{L}_{OTA} = \sum_{k=1}^K \sum_i^N \|\text{sort}(\theta_k^\top f_{dec}^{s(i)}) - \text{sort}(\theta_k^\top f_{dec}^{t(i)})\|_2^2, \quad (6)$$

where $\text{sort}(\cdot)$ is the sorting function that ranks the elements from small to big values, $f_{dec}^{s(i)}, f_{dec}^{t(i)}$ are the i^{th} decoder feature from source and target domains. The projection vector θ_k maps the decoder features into one-dimensional space, i.e., $\theta_k^\top f_{dec}^{s(i)}, \theta_k^\top f_{dec}^{t(i)} \in \mathbb{R}^1$. Hence, we in fact solve the one-dimensional optimal transport problems by optimizing Eq. (6), which have closed-form solutions. Consequently, the domain gap on decoder features will be effectively reduced and the retention for location information is achieved. As validated in 4.5, OTA facilitates the detector to generate highly accurate bounding boxes.

3.3. Total Loss

Here, we introduce the total loss involved to train our method. First, the supervised detection loss is employed on source labeled data for learning the source knowledge. Second, the adaptation losses, i.e., the losses of OAA and OTA modules are applied for facilitating the knowledge transfer from source to target domains. The overall loss of ours:

$$\mathcal{L} = \mathcal{L}_{det} + \mathcal{L}_{OAA} + \beta \mathcal{L}_{OTA} \quad (7)$$

where \mathcal{L}_{det} is the supervised detection loss on source domain, β is the trade-off hyper-parameter.

4. Experiments

In this section, we conduct extensive experiments on several cross-domain object detection benchmarks for verifying the effectiveness of our method. An ablation study and visualization analysis are presented for validating the design of ours.

4.1. Experiment Setup

The following datasets are adopted for evaluation: **Cityscapes**. The Cityscapes [7] is composed of city scene images. The training set of Cityscapes contains 2,975 images while the validation set has 500 images. We adopt the validation set to test methods when Cityscapes is the target domain. **Foggy Cityscapes**. Foggy Cityscapes [36] is the fog version of Cityscapes by applying fog synthesis algorithm on the original Cityscapes images for generating foggy images. Thus, Foggy Cityscapes and Cityscapes share identical annotations. **Sim10k**. Powered by the game engine of Grand Auto Theft, Sim10k [21] contains 10,000 generated images of the game scenes as well as 58,701 annotations for cars. The images of Sim10k can be leveraged to construct the synthetic to real adaption scenario. **BDD100k**. BDD100k [47] includes 70,000 training images and 10,000 validation images. The subset of BDD100k that contains *daytime* images is selected to construct the adaptation benchmark. Thus, we use 36,728 images for training and 5,258 images for validation.

With the aforementioned datasets, we build three adaptation scenarios: weather adaption (Cityscapes \rightarrow Foggy Cityscapes), synthetic to real adaptation (sim10k \rightarrow Cityscapes) and scene adaptation (Cityscapes \rightarrow BDD100k). Following DAF [33], we report the results of mean Average Precision (mAP) with a threshold 0.5.

4.2. Implementation Details

We adopt the Deformable DETR [51] with a ImageNet [11] pre-trained ResNet-50 [16] backbone as the based detector. Inherited from the original paper [51], the learning rate of Deformable DETR is set as 2×10^{-4} and the Adam optimizer [24] is used for updating parameters. The learning rate of the domain discriminator adopted in OAA module is 4×10^{-3} . As [20,], we pre-train models on source domain for a reliable initialization for pseudo labels. The threshold τ is set as 0.5 for all experiments. λ and β are both 1 on Cityscapes \rightarrow Foggy Cityscapes, and 0.1 on the rest.

4.3. Comparisons with SOTA Methods

Weather adaptation. Handling varying weather is crucial and frequent in autonomous driving. Thus, we evaluate our method on Cityscapes \rightarrow Foggy Cityscapes. Table 2 shows the results, from which one can observe that ours significantly exceeds others, validating that the two proposed

Table 2. Results on weather adaption scenario , i.e., Cityscapes \rightarrow Foggy Cityscapes. D-DETR denotes Deformable DETR [51].

Method	Detector	person	rider	car	truck	bus	train	mcycle	bicycle	mAP
Faster RCNN (source)	Faster RCNN	26.9	38.2	35.6	18.3	32.4	9.6	25.8	28.6	26.9
DAF [6]	Faster RCNN	29.2	40.4	43.4	19.7	38.3	28.5	23.7	32.7	32.0
DivMatch [23]	Faster RCNN	31.8	40.5	51.0	20.9	41.8	34.3	26.6	32.4	34.9
SWDA [35]	Faster RCNN	31.8	44.3	48.9	21.0	43.8	28.0	28.9	35.8	35.3
SCDA [50]	Faster RCNN	33.8	42.1	52.1	26.8	42.5	26.5	29.2	34.5	35.9
MTOR [2]	Faster RCNN	30.6	41.4	44.0	21.9	38.6	40.6	28.3	35.6	35.1
CR-DA [44]	Faster RCNN	30.0	41.2	46.1	22.5	43.2	27.9	27.8	34.7	34.2
CR-SW [44]	Faster RCNN	34.1	44.3	53.5	24.4	44.8	38.1	26.8	34.9	37.6
GPA [45]	Faster RCNN	32.9	46.7	54.1	24.7	45.7	41.1	32.4	38.7	39.5
D-adapt [20]	Faster RCNN	40.8	47.1	57.5	33.5	46.9	41.4	33.6	43.0	43.0
ViSGA [34]	Faster RCNN	38.8	45.9	57.2	29.9	50.2	51.9	31.9	40.9	43.3
FCOS (source)	FCOS	36.9	36.3	44.1	18.6	29.3	8.4	20.3	31.9	28.2
EPM [18]	FCOS	44.2	46.6	58.5	24.8	45.2	29.1	28.6	34.6	39.0
KTNNet [38]	FCOS	46.4	43.2	60.6	25.8	41.2	40.4	30.7	38.8	40.9
Deformable DETR (source)	D-DETR	38.0	38.7	45.3	16.3	26.7	4.2	22.9	36.7	28.6
SFA [42]	D-DETR	46.5	48.6	62.6	25.1	46.2	29.4	28.3	44.0	41.3
Ours	D-DETR	48.7	51.5	63.6	31.1	47.6	47.8	38.0	45.9	46.8

Table 3. Results on scene adaptation scenario, i.e., Cityscapes \rightarrow BDD100k. D-DETR denotes Deformable DETR [51].

Method	Detector	person	rider	car	truck	bus	mcycle	bicycle	mAP
Faster R-CNN (source)	Faster RCNN	28.8	25.4	44.1	17.9	16.1	13.9	22.4	24.1
DAF [6]	Faster RCNN	28.9	27.4	44.2	19.1	18.0	14.2	22.4	24.9
SWDA [35]	Faster RCNN	29.5	29.9	44.8	20.2	20.7	15.2	23.1	26.2
SCDA [50]	Faster RCNN	29.3	29.2	44.4	20.3	19.6	14.8	23.2	25.8
CR-DA [44]	Faster RCNN	30.8	29.0	44.8	20.5	19.8	14.1	22.8	26.0
CR-SW [44]	Faster RCNN	32.8	29.3	45.8	22.7	20.6	14.9	25.5	27.4
FCOS [39] (source)	FCOS	38.6	24.8	54.5	17.2	16.3	15.0	18.3	26.4
EPM [18]	FCOS	39.6	26.8	55.8	18.8	19.1	14.5	20.1	27.8
Deformable DETR (source)	D-DETR	38.9	26.7	55.2	15.7	19.7	10.8	16.2	26.2
SFA [42]	D-DETR	40.2	27.6	57.5	19.1	23.4	15.4	19.2	28.9
Ours	D-DETR	40.4	31.2	58.6	20.4	25.0	14.9	22.7	30.5

alignment modules can indeed mitigate the domain shift under the variation of weather conditions.

Synthetic to real adaptation. Adopting synthetic images for training is economical, saving the cost of collecting and annotating data. Sim10k \rightarrow Cityscapes reflects how well the model adapted from synthesis to real domains. Table 1 shows that our method achieves promising performance improvement over other methods.

Scene adaptation. When the layout of scene varies in different cities, the performance might drop. To test the robustness to the layout variation, we carry out the experiments on Cityscapes \rightarrow BDD100k as shown in the Table 3. Our proposed method consistently improves the source model, validating our alignment strategy is general to scene adaption.

4.4. Ablation Study

To validate each component of our method, we conduct ablation study on Cityscapes \rightarrow Foggy Cityscapes (see Table 4). We build our method by adding components to the source model. First, by adding object-aware alignment

(OAA), the detection performance significantly improves, manifesting the importance of aligning backbone features. Second, we only add the decoder alignment module (OTA), the performance gain is not as impressive as that brought by backbone alignment module. The reason is that the biased backbone features severely hinder the adaptation of the following transformer. Via adding both the alignment modules, we reach our proposed method, which yields the best performance. One could observe that the two alignment modules are complementary to each other. OAA provides domain-invariant based features for the following process while the OTA further reduces the domain gap on the decoder features that are directly utilized for final detections.

In addition, we analyze the two modules by introducing their variations, i.e., global backbone alignment (GA) and adversarial decoder alignment (ADA). The former indeed can enhance the model performance but will be more powerful when cooperating with the pseudo bounding boxes for emphasizing the foreground regions. On the other hand, the latter achieves inferior results compared with the OTA, demonstrating that adversarial learning might distort the lo-

Table 4. Ablation study on Cityscapes \rightarrow Foggy Cityscapes. OAA and OTA denote the proposed Object-Aware Alignment and Optimal Transport based Alignment modules. GA and ADA indicate global alignment on backbone features and adversarial alignment on decoder features.

Methods	OAA	OTA	GA	ADA	person	rider	car	truck	bus	train	mcycle	bicycle	mAP
Deformable DETR (source)					38.0	38.7	45.3	16.3	26.7	4.2	22.9	36.7	28.6
Proposed	✓				45.8	48.7	61.2	30.4	48.3	33.5	34.0	43.1	43.1
		✓			46.2	47.5	61.9	24.1	45.9	29.2	25.1	41.8	40.2
		✓	✓		47.4	49.3	63.8	28.9	46.5	32.6	32.1	44.7	43.2
	✓			✓	48.3	50.5	65.0	30.7	49.5	34.5	34.6	44.3	44.7
Ours	✓	✓			48.7	51.5	63.6	31.1	47.6	47.8	38.0	45.9	46.8

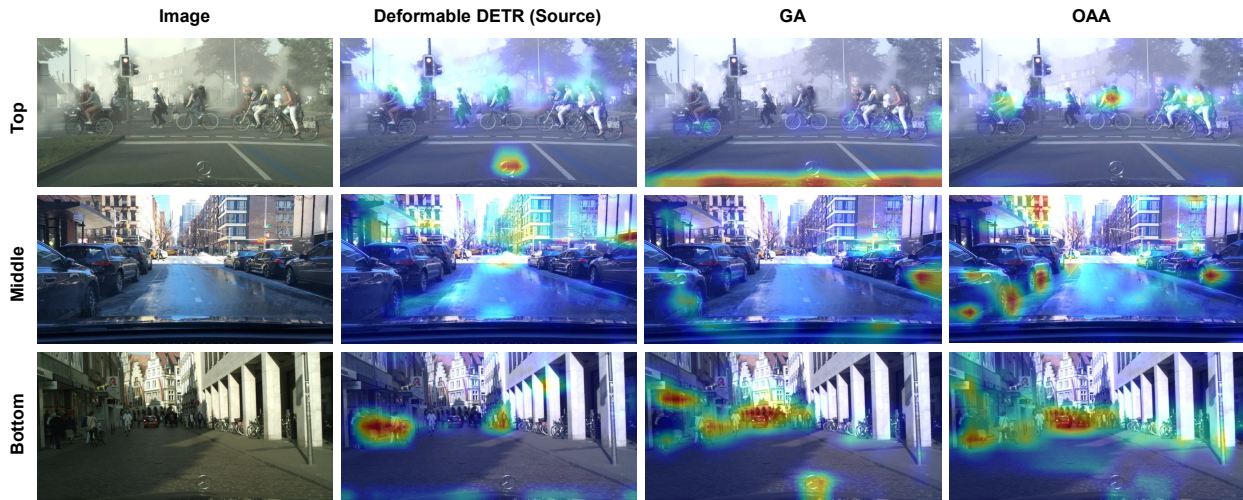


Figure 4. Illustration of the attention maps for testing samples. We presented the attention maps of three methods, i.e., Deformable DETR (source), Global Alignment (GA) and our Object-Aware Alignment (OAA) on backbone features. From top to bottom, we exhibit the testing examples from Cityscapes \rightarrow Foggy Cityscapes, Cityscapes \rightarrow BDD100k and Sim10k \rightarrow Cityscapes.

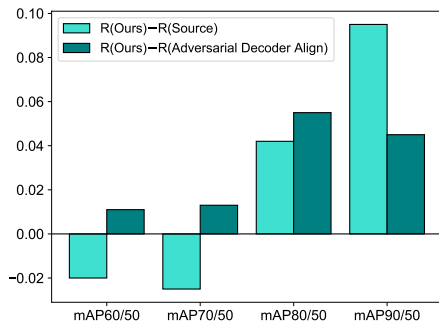


Figure 5. The difference of the mAP ratio (R) that measures the percentage of highly accurate predicted bounding boxes in all accurate bounding boxes. For example, mAP70/50 indicates the portion of predicted bounding boxes with $\text{IOU} \geq 0.7$ in the predicted bounding boxes with $\text{IOU} \geq 0.5$. “R(Ours)−R(Source)” denote the map ratios of ours minus the map ratios of the source model.

cation information, resulting in limited performance.

4.5. Analytical Experiments

Attention visualization. To analyze why Object-Aware Alignment module improves the detection performance, we

visualize the attention maps of the CNN backbone features extracted by the plain source model, the source models with global alignment and OAA in Fig. 4. Via global alignment, the model put more attention on the objects, since the detection knowledge is partial transfer to the target domain. While, OAA can further facilitate the attention for objects and decrease the attention on background areas, thanks to the mechanism that utilizes the pseudo boxes for highlighting the foreground regions.

Analysis of highly accurate bounding boxes. To narrow the domain gap while avoiding distorting the intrinsic location information on decoder features, we utilize the sliced Wasserstein Distance to decrease the domain discrepancy. We illustrate how exactly precise are the bounding boxes considered to be true positive by calculating the portion of highly accurate boxes in all the boxes with $\text{IOU} \geq 0.5$. And we show the difference of this mAP ratio between Ours and Others. From Fig. 5, one can observe that our method consistently makes more highly-accurate box predictions than others, especially when the criterion is critical, i.e., mAP90/50 and mAP80/50.

Detection results. We illustrate some detection results of source model, SFA [42] and ours, and the ground-truth

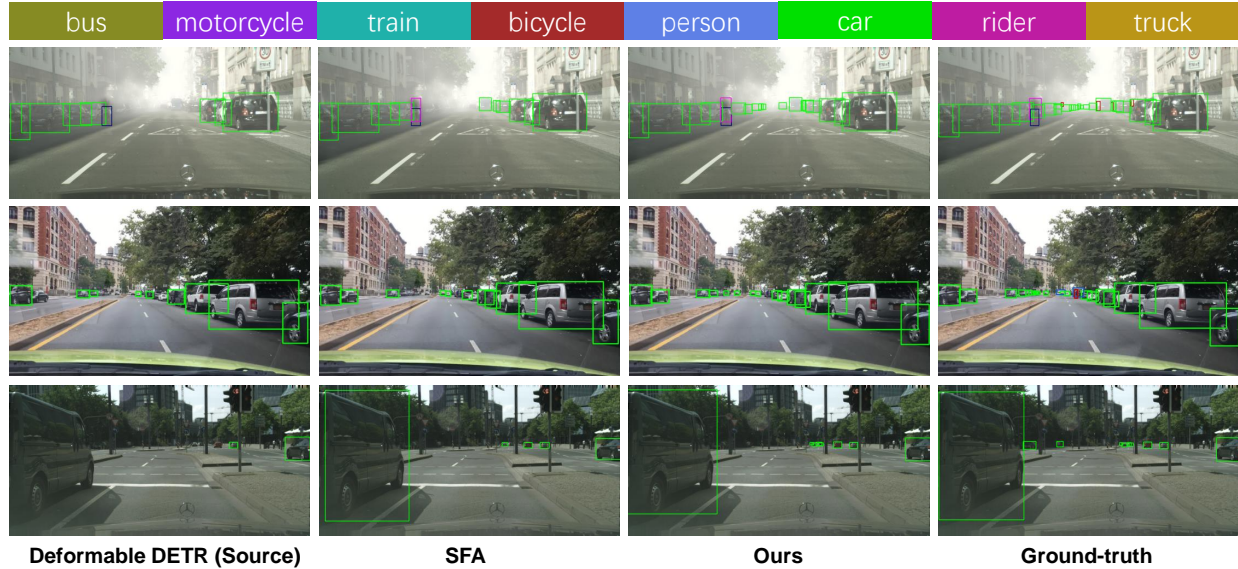


Figure 6. Qualitative results: Top, middle and bottom exhibit the visualization detection results of adaptation scenario Cityscapes \rightarrow Foggy Cityscapes, Cityscapes \rightarrow BDD100k and Sim10k \rightarrow Cityscapes.

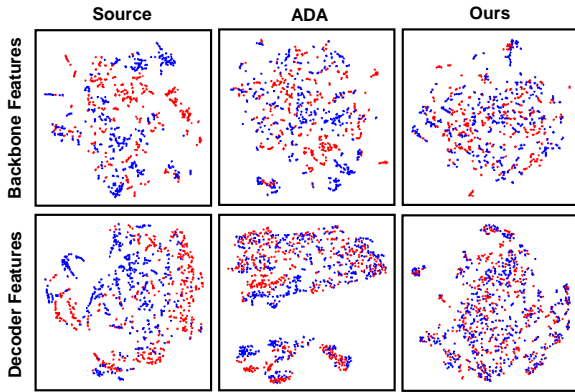


Figure 7. t-SNE [41] visualization of the features of CNN backbone and decoder. The red and blue dots denote the features from source and target domains, respectively. Adversarial decoder alignment (ADA) indicates that utilizing adversarial training to align the features of decoder.

boxes in Fig. 6. Ours significantly reduce the false negatives, i.e., detecting the objects that aren’t detected by other methods, validating the effectiveness of our proposed two alignment modules that can effectively close the domain gap. In addition, our method shows advanced performance on small objects. This manifests that aligning multi-scale backbone features is more effective for detecting the small object than aligning the encoder embeddings. This might stem from that the backbone features contain more details about small objects.

Feature Visualization. Utilizing t-SNE [41], we visualize the feature distributions of CNN and decoder from two domains, as shown in Fig. 7. The features of the source model are separated by domains, while our method aligns the features of two domains on both CNN backbone and

decoder, thus achieving performance gains. In addition, the decoder features do not have an obvious cluster property since they carry location information. On the other hand, adversarial decoder alignment compresses the feature distribution of decoder, which might damage the intrinsic location information.

5. Conclusion

In this work, we delve into the problem of adapting the DETR-style detector to new domains. We build our method based on two findings, introducing an Object-Aware Alignment module for align the multi-scale backbone features, and an Optimal Transport based Alignment module for reduce the domain gap on decoder features and maximumly preserve the localization information. Both modules contribute to the promising performance of our method.

References

- [1] Martin Arjovsky, Soumith Chintala, and Léon Bottou. Wasserstein generative adversarial networks. In *ICML*, pages 214–223. PMLR, 2017. 4
- [2] Qi Cai, Yingwei Pan, Chong-Wah Ngo, Xinmei Tian, Lingyu Duan, and Ting Yao. Exploring object relation in mean teacher for cross-domain detection. In *CVPR*, pages 11457–11466, 2019. 3, 6, 7
- [3] Nicolas Carion, Francisco Massa, Gabriel Synnaeve, Nicolas Usunier, Alexander Kirillov, and Sergey Zagoruyko. End-to-end object detection with transformers. In *ECCV*, pages 213–229. Springer, 2020. 1, 3
- [4] Chaoqi Chen, Zebiao Zheng, Yue Huang, Xinghao Ding, and Yizhou Yu. I3net: Implicit instance-invariant network for adapting one-stage object detectors. In *IEEE Conference on*

- Computer Vision and Pattern Recognition, CVPR 2021, virtual, June 19-25, 2021*, pages 12576–12585. Computer Vision Foundation / IEEE, 2021. 3
- [5] Xinyang Chen, Sinan Wang, Mingsheng Long, and Jianmin Wang. Transferability vs. discriminability: Batch spectral penalization for adversarial domain adaptation. In *ICML*, pages 1081–1090. PMLR, 2019. 2, 5
 - [6] Yuhua Chen, Wen Li, Christos Sakaridis, Dengxin Dai, and Luc Van Gool. Domain adaptive faster r-cnn for object detection in the wild. In *CVPR*, pages 3339–3348, 2018. 3, 6, 7
 - [7] Marius Cordts, Mohamed Omran, Sebastian Ramos, Timo Rehfeld, Markus Enzweiler, Rodrigo Benenson, Uwe Franke, Stefan Roth, and Bernt Schiele. The cityscapes dataset for semantic urban scene understanding. In *CVPR*, pages 3213–3223, 2016. 6
 - [8] Nicolas Courty, Rémi Flamary, Amaury Habrard, and Alain Rakotomamonjy. Joint distribution optimal transportation for domain adaptation. *NeurIPS*, 30, 2017. 4
 - [9] Zhigang Dai, Bolun Cai, Yugeng Lin, and Junying Chen. Up-detr: Unsupervised pre-training for object detection with transformers. In *CVPR*, 2020. 3
 - [10] Bharath Bhushan Damodaran, Benjamin Kellenberger, Rémi Flamary, Devis Tuia, and Nicolas Courty. Deepjdot: Deep joint distribution optimal transport for unsupervised domain adaptation. In *ECCV*, pages 447–463, 2018. 4
 - [11] Jia Deng, Wei Dong, Richard Socher, Li-Jia Li, Kai Li, and Li Fei-Fei. Imagenet: A large-scale hierarchical image database. In *CVPR*, pages 248–255, 2009. 6
 - [12] Jinhong Deng, Wen Li, Yuhua Chen, and Lixin Duan. Unbiased mean teacher for cross-domain object detection. In *CVPR*, pages 4091–4101, 2021. 3
 - [13] R Flamary, N Courty, D Tuia, and A Rakotomamonjy. Optimal transport for domain adaptation. *IEEE Transactions on Pattern Analysis and Machine Intelligence*, 1, 2016. 4
 - [14] Yaroslav Ganin, Evgeniya Ustinova, Hana Ajakan, Pascal Germain, Hugo Larochelle, François Laviolette, Mario Marchand, and Victor Lempitsky. Domain-adversarial training of neural networks. *The journal of machine learning research*, 17(1):2096–2030, 2016. 2
 - [15] Ross Girshick. Fast r-cnn. In *ICCV*, pages 1440–1448, 2015. 3
 - [16] Kaiming He, Xiangyu Zhang, Shaoqing Ren, and Jian Sun. Deep residual learning for image recognition. In *CVPR*, pages 770–778, 2016. 6
 - [17] Zhenwei He and Lei Zhang. Multi-adversarial faster-rcnn for unrestricted object detection. In *ICCV*, pages 6668–6677, 2019. 3
 - [18] Cheng-Chun Hsu, Yi-Hsuan Tsai, Yen-Yu Lin, and Ming-Hsuan Yang. Every pixel matters: Center-aware feature alignment for domain adaptive object detector. In *ECCV*, pages 733–748. Springer, 2020. 3, 6, 7
 - [19] Han-Kai Hsu, Chun-Han Yao, Yi-Hsuan Tsai, Wei-Chih Hung, Hung-Yu Tseng, Maneesh Singh, and Ming-Hsuan Yang. Progressive domain adaptation for object detection. In *WACV*, 2020. 3
 - [20] Janguang Jiang, Baixu Chen, Jianmin Wang, and Mingsheng Long. Decoupled adaptation for cross-domain object detection. *arXiv preprint arXiv:2110.02578*, 2021. 3, 4, 6, 7
 - [21] Matthew Johnson-Roberson, Charles Barto, Rounak Mehta, Sharath Nittur Sridhar, Karl Rosaen, and Ram Vasudevan. Driving in the matrix: Can virtual worlds replace human-generated annotations for real world tasks? In *ICRA*, pages 746–753. IEEE, 2017. 6
 - [22] Seunghyeon Kim, Jaehoon Choi, Taekyung Kim, and Changick Kim. Self-training and adversarial background regularization for unsupervised domain adaptive one-stage object detection. In *ICCV*, pages 6092–6101, 2019. 3, 4
 - [23] Taekyung Kim, Minki Jeong, Seunghyeon Kim, Seokeon Choi, and Changick Kim. Diversify and match: A domain adaptive representation learning paradigm for object detection. In *CVPR*, pages 12456–12465, 2019. 3, 6, 7
 - [24] Diederik P Kingma and Jimmy Ba. Adam: A method for stochastic optimization. In *ICLR*, 2015. 6
 - [25] Chen-Yu Lee, Tanmay Batra, Mohammad Haris Baig, and Daniel Ulbricht. Sliced wasserstein discrepancy for unsupervised domain adaptation. In *CVPR*, pages 10285–10295, 2019. 4
 - [26] Feng Li, Hao Zhang, Shilong Liu, Jian Guo, Lionel M Ni, and Lei Zhang. Dn-detr: Accelerate detr training by introducing query denoising. *arXiv preprint arXiv:2203.01305*, 2022. 3
 - [27] Jian Liang, Dapeng Hu, and Jiashi Feng. Do we really need to access the source data? source hypothesis transfer for unsupervised domain adaptation. In *ICML*, pages 6028–6039. PMLR, 2020. 4
 - [28] Jian Liang, Dapeng Hu, and Jiashi Feng. Domain adaptation with auxiliary target domain-oriented classifier. In *CVPR*, pages 16632–16642, 2021. 4
 - [29] Shilong Liu, Feng Li, Hao Zhang, Xiao Yang, Xianbiao Qi, Hang Su, Jun Zhu, and Lei Zhang. Dab-detr: Dynamic anchor boxes are better queries for detr. *arXiv preprint arXiv:2201.12329*, 2022. 3
 - [30] Wei Liu, Dragomir Anguelov, Dumitru Erhan, Christian Szegedy, Scott Reed, Cheng-Yang Fu, and Alexander C Berg. Ssd: Single shot multibox detector. In *ECCV*, pages 21–37. Springer, 2016. 3
 - [31] Julien Rabin, Gabriel Peyré, Julie Delon, and Marc Bernot. Wasserstein barycenter and its application to texture mixing. In *SSVM*, pages 435–446. Springer, 2011. 4, 5
 - [32] Joseph Redmon, Santosh Divvala, Ross Girshick, and Ali Farhadi. You only look once: Unified, real-time object detection. In *CVPR*, pages 779–788, 2016. 3
 - [33] Shaoqing Ren, Kaiming He, Ross Girshick, and Jian Sun. Faster r-cnn: towards real-time object detection with region proposal networks. *IEEE Transactions on Pattern Analysis and Machine Intelligence*, 39(6):1137–1149, 2016. 3, 6
 - [34] Farzaneh Rezaeianaran, Rakshith Shetty, Rahaf Aljundi, Daniel Olmeda Reino, Shanshan Zhang, and Bernt Schiele. Seeking similarities over differences: Similarity-based domain alignment for adaptive object detection. In *ICCV*, pages 9184–9193. IEEE, 2021. 3, 6, 7

- [35] Kuniaki Saito, Yoshitaka Ushiku, Tatsuya Harada, and Kate Saenko. Strong-weak distribution alignment for adaptive object detection. In *CVPR*, pages 6956–6965, 2019. 3, 6, 7
- [36] Christos Sakaridis, Dengxin Dai, and Luc Van Gool. Semantic foggy scene understanding with synthetic data. *International Journal of Computer Vision*, 126(9):973–992, 2018. 6
- [37] Jian Shen, Yanru Qu, Weinan Zhang, and Yong Yu. Wasserstein distance guided representation learning for domain adaptation. In *AAAI*, 2018. 4
- [38] Kun Tian, Chenghao Zhang, Ying Wang, Shiming Xiang, and Chunhong Pan. Knowledge mining and transferring for domain adaptive object detection. In *ICCV*, pages 9113–9122. IEEE, 2021. 6, 7
- [39] Zhi Tian, Chunhua Shen, Hao Chen, and Tong He. Fcos: Fully convolutional one-stage object detection. In *ICCV*, pages 9627–9636, 2019. 7
- [40] Hugo Touvron, Matthieu Cord, Matthijs Douze, Francisco Massa, Alexandre Sablayrolles, and Hervé Jégou. Training data-efficient image transformers & distillation through attention. In *ICML*, pages 10347–10357. PMLR, 2021. 1
- [41] Laurens Van der Maaten and Geoffrey Hinton. Visualizing data using t-sne. *Journal of machine learning research*, 9(11), 2008. 9
- [42] Wen Wang, Yang Cao, Jing Zhang, Fengxiang He, Zheng-Jun Zha, Yonggang Wen, and Dacheng Tao. Exploring sequence feature alignment for domain adaptive detection transformers. In *ACM MM*, pages 1730–1738, 2021. 1, 2, 6, 7, 8
- [43] Shaoan Xie, Zibin Zheng, Liang Chen, and Chuan Chen. Learning semantic representations for unsupervised domain adaptation. In *ICML*, pages 5423–5432. PMLR, 2018. 4
- [44] Chang-Dong Xu, Xing-Ran Zhao, Xin Jin, and Xiu-Shen Wei. Exploring categorical regularization for domain adaptive object detection. In *CVPR*, pages 11724–11733, 2020. 3, 6, 7
- [45] Minghao Xu, Hang Wang, Bingbing Ni, Qi Tian, and Wenjun Zhang. Cross-domain detection via graph-induced prototype alignment. In *CVPR*, pages 12355–12364, 2020. 3, 6, 7
- [46] Jason Yosinski, Jeff Clune, Yoshua Bengio, and Hod Lipson. How transferable are features in deep neural networks? In *NeurIPS*, 2014. 2
- [47] Fisher Yu, Wenqi Xian, Yingying Chen, Fangchen Liu, Mike Liao, Vashisht Madhavan, and Trevor Darrell. Bdd100k: A diverse driving video database with scalable annotation tooling. *arXiv preprint arXiv:1805.04687*, 2(5):6, 2018. 6
- [48] Hao Zhang, Feng Li, Shilong Liu, Lei Zhang, Hang Su, Jun Zhu, Lionel M Ni, and Heung-Yeung Shum. Dino: Detr with improved denoising anchor boxes for end-to-end object detection. *arXiv preprint arXiv:2203.03605*, 2022. 3
- [49] Yixin Zhang, Zilei Wang, and Yushi Mao. RPN prototype alignment for domain adaptive object detector. In *CVPR*, pages 12425–12434, 2021. 3, 6
- [50] Xinge Zhu, Jiangmiao Pang, Ceyuan Yang, Jianping Shi, and Dahua Lin. Adapting object detectors via selective cross-domain alignment. In *CVPR*, pages 687–696, 2019. 3, 6, 7
- [51] Xizhou Zhu, Weijie Su, Lewei Lu, Bin Li, Xiaogang Wang, and Jifeng Dai. Deformable detr: Deformable transformers for end-to-end object detection. In *ICLR*, 2020. 1, 2, 3, 4, 6, 7
- [52] Yang Zou, Zhiding Yu, BVK Kumar, and Jinsong Wang. Unsupervised domain adaptation for semantic segmentation via class-balanced self-training. In *ECCV*, pages 289–305, 2018. 4